Polymeric Friction Modifiers: Influence of Anchoring Chemistry on their Adsorption and Effectiveness

Sébastien Delamarre, Tobias A Gmür, Nicholas D Spencer, Juliette Cayer-Barrioz

Polymeric Friction Modifiers: Influence of Anchoring Chemistry on their Adsorption and Effectiveness

Sébastien Delamarre[1], Tobias Gmür[2], Nicholas D. Spencer[2], Juliette Cayer-Barrioz[1,*]

[1)] Laboratoire de Tribologie et Dynamique des Systèmes, CNRS UMR 5513, Ecole Centrale de Lyon, 36 Avenue Guy de Collongue, 69134 Ecully Cedex, France

[2)] Laboratory for Surface Science and Technology, Department of Materials, ETH Zürich, Vladimir-Prelog-Weg 5, 8093 Zurich, Switzerland

Abstract

Correlated adsorption and lubricity have been investigated using polymeric friction modifiers, specifically designed with an oleophilic-brush-forming block and an anchoring block of comparable length. Through adsorption, rheology and friction measurements, we have highlighted the existence of boundary layers, whose molecular organization and mechanical properties govern the frictional behavior. We have demonstrated that changing the anchoring chemistry controls the final ordering in the boundary layer. The stability of the surface anchoring governs the onset of repulsion between the polymer layers as well as the capacity of the layer to withstand shear. The higher molecular order provided by the most firmly anchored polymer to the surface, was thereby responsible for the significant friction reduction observed.

Introduction

Reducing frictional (and thus energy) dissipation in contacts by adsorbing molecules onto sliding surfaces is not a novel idea. Nevertheless, low-viscosity fluids are increasingly being used to lower frictional energy losses in automobile engines under (elasto)hydrodynamic conditions. As a consequence, ever thinner films [1] are now separating contacting surfaces in most applications. This has resulted in a renewed interest in further reducing friction between the surfaces themselves.

Many different friction-modifier molecules have been designed and applied, ranging from organic friction modifiers to functionalized polymers. Extensive literature [2-11] can be found on organic acids as friction modifiers: these surfactant molecules generally consist of a hydrophilic, polar carboxylic acid group on the end of a lipophilic chain. For relatively short (<20 carbons) linear hydrocarbons chains, Hardy [2] showed that the molecules act by forming a more or less dense monolayer on the surface with the carboxylic acid group physically or chemically adsorbed onto the surface. Once two such covered surfaces are brought into contact and sheared, the shear plane then localized in the picometer-thin zone in which hydrocarbon end-chains of both surfaces interact. The molecular ordering plays a key role in this process and further studies [4-6, 9-11] have shown that the existence of unsaturation in the chain, for instance, can disturb that molecular organization and hence the frictional response. Other anchors, such as amines, have also been investigated (see [5, 10, 12] amongst others) confirming the relation between anchor group, organization, and the ability to reduce friction: for instance, the monolayer formed with a N-alkyl dioleate diamine almost fully covers a metallic surface (saturation surface coverage of 94%) and induces a drastic friction reduction,

down to friction coefficients of a few thousandths, by combining low stiffness in the shear direction with a very thin interpenetration zone [5].

For polymers, the chains are longer and the architecture often very different from the short linear molecules. Polymer additives have routinely been used to modify the temperature-viscosity properties of the lubricant. Nevertheless, polymers also interact with the surface to form thicker boundary films than surfactants. Past studies showed that these boundary films modified the lubricant film separating the surfaces and were also likely to modify the friction response [8, 10, 13-19]. To better control the adsorption, block copolymers have been preferred to random ones [13, 18-19]. The architecture and the chemical nature of the polymers also plays a role on the boundary film formation and friction reduction capability, as shown in [18-19].
In the case of olefinic copolymers, the presence of a functional group lead to the formation of a dense, homogeneous and more elastic polymer layer on the surface [20]. The formation of this few-nanometer-thick boundary film associated with a reduction of friction has also been observed for functionalized polymethacrylates of various molecular weights [21-22]. The mechanisms of friction reduction involve the formation of a more viscous surface layer [13]. However, one can expect an additional viscoelastic contribution of the adsorbed film, at low sliding velocity [10].

First attempts have also been made to identify the polymer configuration and its correlation with the friction mechanisms for commercial polymers with partially unknown chemistry [15-16] and for grafting-from polymerization techniques [17] that do not provide contact replenishment.

The goal of this paper is to investigate the role of the anchoring chemistry of model block copolymer friction modifiers on their capability to form a boundary film on a metallic surface and to reduce friction in a low-viscosity solvent. The polymers have been designed with a brush-forming block and an anchoring block of comparable lengths, with the aim of ensuring strong interaction with the surface, monolayer brush coverage and thus high lubricity. A combined approach using adsorption characterization and friction analysis of the boundary film, by means of the quartz-crystal microbalance (QCM) and the ATLAS tribometer, respectively, was carried out with two different anchoring chemistries: carboxylic acid or primary amine. While these moieties are both capable of interacting electrostatically with transition-metal surfaces and their oxides, carboxylic acid groups have previously been shown to exhibit stronger, bidentate interactions [23].

Experimental section

Fluids

Polymer solutions were prepared at 0.5%w/w in hexadecane. Hexadecane was purchased from Sigma-Aldrich at 99% purity. Its viscosity, measured with an Anton Paar MCR302 Rheometer with double-wall accessory (DG26.7 with 2 mm gap) at 25°C, over a shear rate from 30 s^{-1} to 3000 s^{-1}, was 3 mPa.s. The polymers were synthesized according to [18-19], via controlled radical polymerization and active-ester postfunctionalization, to yield a precise architecture with differing anchoring chemistries. Gel-permeation chromatography (GPC) measurements were performed on a Viscotek GPC system (Malvern Panalytical Ltd, UK) equipped with a pump and degasser (GPCmax VE2001, 1.0ml/min flow rate), a differential-refractometer detector module (Viscotek 302 TDA) and a mixed bed column (2x PLgel5 μm MIXED, 300 x 7.5 mm) using THF as an eluent. The final polymers consisted of an oleophilic block of 10.5

nm in length and a 9-nm-long, surface-active anchoring block. The latter block had been modified to yield different anchoring moieties such as primary amine in the case of polymer Pol-Amine and carboxylic acid in the case of Pol-Carbox [18]. The pre-functionalized p12MA-b-pPFPAc had a molecular mass, Mn = 21.3 kDa with a PDI of 1.16.

Dynamic Light Scattering (DLS) was performed using a Malvern Zetasizer Nano ZS to characterize the micellar diameter of the polymeric solutions [18]. Averaged values over 6 repeat measurements at 25°C are reported in **Table 1**, which indicates the presence of rather large micelles in solution.

Table 1: Experimental details – micellar diameters and cobalt sphere radii

Fluid	Hexadecane	Pol-Carbox solution	Pol-Amine solution
D_{av} ($x10^{-9}$ m)		21 ± 0	44 ± 0
R ($x\ 10^{-3}$ m)	2.36 ± 0.01	2.26 ± 0.01	2.28 ± 0.01

Quartz-Crystal Microbalance

Adsorption measurements were carried out using a QCM-D E4 (Biolin Scientific AB, Sweden) at 25°C with iron oxide coated substrates (QSX 326, Fe_3O_4, used only once and freshly out of the box). These surfaces were cleaned in an ultrasonic bath for 20 min in ethanol, before being rinsed with ultrapure water and blown dry with filtered nitrogen [19]. The rest of the measurement setup was cleaned by sonication in isopropanol and hexane. Each of the four cells was connected in parallel to a peristaltic pump and rinsed with hexadecane for 4 h for equilibration at a constant flow rate of 2.5 µl/s per sensor. The measurement itself consisted of 20 min further equilibration, after which the lubricant solution reservoir was connected for 20 min, and the cells finally purged with pure hexadecane again for 20 min.

The measured frequency and dissipation shifts were analyzed with the Sauerbrey equation [24], as the criteria for applicability of [25] was met. The resulting mass was transformed for comparison with the remaining measurements, assuming a density of 0.77 $g.cm^{-3}$ as in the bulk liquid.

ATLAS Tribometer

A fused-silicate glass sphere of radius, R, and a <111> silicon wafer were both coated with a 3-nm cobalt layer using cathodic sputtering under low argon pressure (10^{-6} mbar), in order to use chemically symmetrical metallic surfaces. This conductive coating permits the absolute origin of distance to be precisely defined, as explained in [26-27], by means of sphere/plane capacitance measurements. The existence of a 0.3 nm thick oxide layer on top of the cobalt surfaces was previously measured by X-ray photoelectron spectroscopy [26]. After the experiments, the rms roughness of both surfaces was measured at about 0.5 nm ± 0.3 nm by interferometry over 47× 63 μm^2 and AFM over 1× 1 μm^2. No surface damage was detected. The values of radius, R, are reported in **Table 1**.

The ATLAS molecular tribometer, whose principle is described in detail in [27], was used to carry out squeeze and friction experiments on a lubricated sphere/plane contact.

Quasi-static and dynamic displacements of the sphere were imposed in three dimensions via piezoelectric actuators. Displacements and forces were simultaneously and independently measured by means of high-resolution capacitive sensors [27].

A set of surfaces was prepared for each experiment (see [26] for details in the surface preparation and cleanliness checks). The values of sphere radii are reported in **Table 1**. Experiments were performed at 25 ± 0.5 °C under 1 bar of argon. A droplet of polymer solution

was deposited between the two surfaces and left for 1-3 min before rinsing twice with hexadecane that had been dehydrated with zeolites for several days before use, as preliminary QCM experiments showed that the adsorption only took a few seconds [18].

This experimental protocol was defined in order to investigate the role of the anchor chemistry on surface organization and frictional behavior, while avoiding any interference by potential micelles in the bulk solution.

Boundary-film formation and characterization were investigated by carrying out squeeze experiments at a closing speed of 0.1 $nm.s^{-1}$ with superimposed oscillations in the z and x directions at 38 Hz and 70 Hz, and small amplitudes of ±0.35 nm and ±0.15 nm, respectively. The evolution of the normal force, Fz, as a function of the sphere/plane separation distance, was analyzed in order to characterize the boundary film under confinement. Dynamic measurements of displacements and forces provided simultaneous information on interfacial film rheology, in terms of damping and stiffness, in both normal (z) and tangential (x) directions.

The friction behavior and the evolution of the friction force, Fx, were investigated at constant normal force, Fz, which was either equal to 1 mN or 3 mN for sliding velocity, V_x, values ranging from 0.1 to 100 $nm.s^{-1}$. The values of friction force are averaged over at least 4 steady-state measurements.

Results and discussion

Adsorption

QCM-D results covered three, distinct periods during measurements (**Fig. 1**): during the first 25 minutes there was a constant flow of hexadecane, which allowed the baseline to be obtained; the following 20 minutes corresponded to the polymer solutions reaching the sensor cells; the last 20 minutes were recorded during hexadecane rinsing. Both polymer solutions exhibited a residual change in frequency shift ΔFn/n signal following hexadecane rinsing, meaning that polymer molecules were irreversibly bonded to the surface. The evolution of the dissipation signals, ΔD, showed a degree of reversibility: the values increased drastically after introduction of the polymer solutions and decreased significantly after rinsing, implying that the residual films did not exhibit significant viscous dissipation—an indication of rigidity [18].

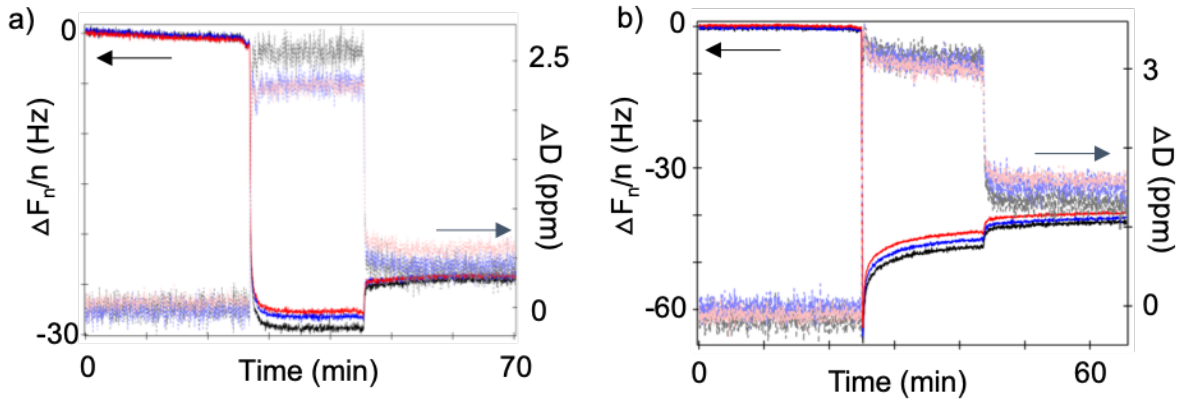

Fig. 1: QCM-D raw data results for polymers Pol-Carbox (a) and Pol-Amine (b).

Boundary-film formation

Solvent

The hydrodynamic flow for pure hexadecane was analyzed at large separations by taking dynamic measurements while squeezing. Assuming a viscous behavior and fluid adherence to the surfaces, the inverse of the normal damping presented in **Fig 2a** (dark blue curves), followed Stokes's law with a bulk viscosity of 3.2 mPa.s, in agreement with the bulk viscometer measurement. In the presence of adsorbed layers, flow conditions are shifted by a hydrodynamic length, $L_н$, corresponding to molecules adsorbed on each surface [28]. This immobile layer of infinite viscosity does not participate in the flow [28]. $L_н$ for hexadecane was determined to be 1.35 ± 0.2 nm, as shown in **Fig 2b**, corresponding to a few layers of hexadecane molecules lying down on the surfaces [19]. Reversible behavior was measured upon loading and unloading (see **Fig 2a**).

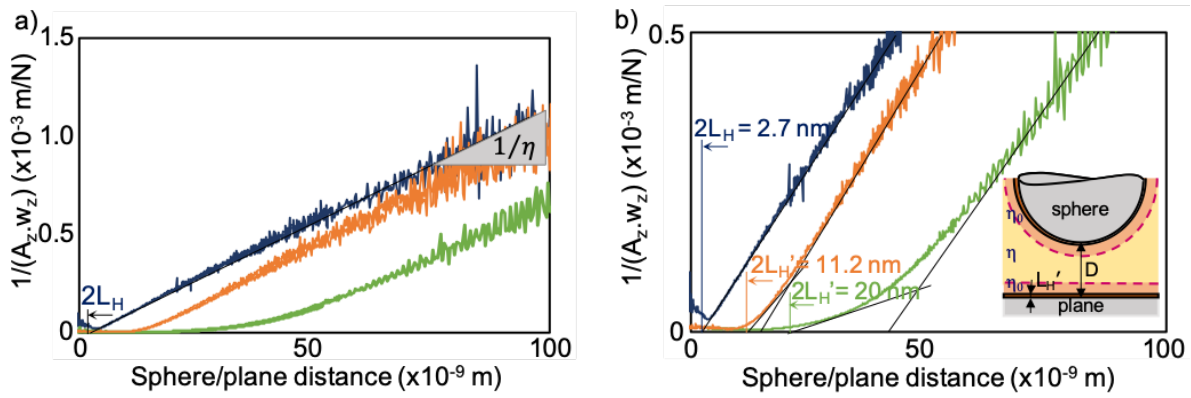

Fig. 2: Superimposed approach and retraction curves showing the inverse of the normal damping a) at large distances, b) zoom on smaller values of the inverse of the normal damping, for hexadecane (blue), Pol-Carbox + hexadecane (orange) and Pol-Amine + hexadecane (green). These curves were obtained using the dynamic measurements during a

squeeze experiment. The viscosity is obtained from the reciprocal of the slope according to Stokes' law and the values of the immobile layer thickness, L_{ni}, and L_{ni}', the corresponding length for the interfaces with adsorbed polymers, can be extrapolated from the intercept with the x-axis. The schematic in (b) represented a tentative description of the multilayering interface for the two polymers.

At smaller sphere/plane separation distances, the normal force F_z/R sharply increases while the distance remains more or less constant, indicating the existence of an elastic wall (see **Fig 3**). The thickness of this wall is equal to $2L_c$ (1mN) = 2.5 nm and $2L_c$ (3mN) = 2 nm. Lc corresponds to the thickness of the confined layer on each surface. The normal force does not increase continuously, but rather in small steps of amplitude 0.1-0.2 nm. This indicates a high stiffness in the normal direction combined with hexadecane molecular rearrangements under confinement. This is also confirmed by the small hysteresis between loading and unloading. The normal force is repulsive during loading and slightly adhesive during unloading with an adhesive force F_0 = 0.014 mN. This allows the contact mechanics to be modelled, to account for the elastic deformation of the solids, as explained in detail in [28], and the corresponding contact pressure to be calculated: here 44 MPa for F_z = 3 mN. The high normal stiffness can also be attributed to the existence of a solidified layer as the solidification pressure of hexadecane is about 25 MPa at 23.5°C [29]. The steps could then be attributed to the motion of stacking defects during loading, as seen previously in the literature [30-31].

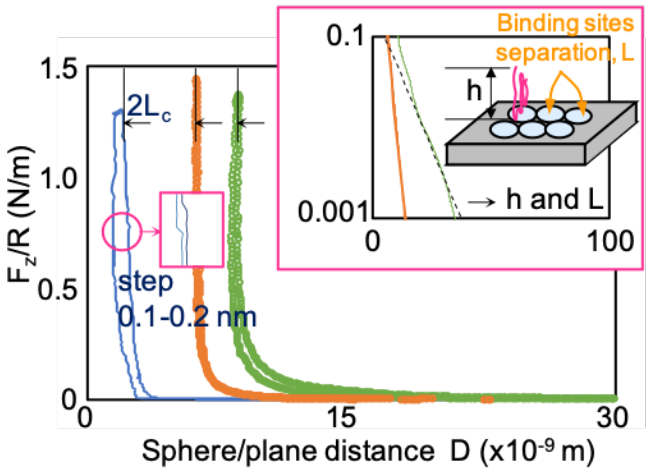

Fig. 3: Evolution of the normal force, F_z/R, as a function of the distance D, during a quasi-static squeeze experiment, for hexadecane (blue), Pol-Carbox + hexadecane (orange) and Pol-Amine + hexadecane (green). The inset shows the repulsive force at large distance for the two polymer solutions with the meaning of h and L defined in the schematic, h being the length of first repulsion and L the binding-site separation.

During loading, the tangential stiffness K_x increases to reach 160 000 $N.m^{-1}$ at maximum normal force. It reversibly decreases during unloading (see **Fig 4**). From these measurements, the elastic shear modulus can be calculated [28, 32] as 4.3 MPa, assuming infinitely rigid solids, and 6.9 MPa accounting for the solid substrate elasticity. These values are reported in **Table 2**.

This measurement of the interfacial film thickness for the solvent, L_c, showed that it was very close in value to L_H (L_H/L_c(1mN) = 0.93), consistent with a saturation surface coverage [33].

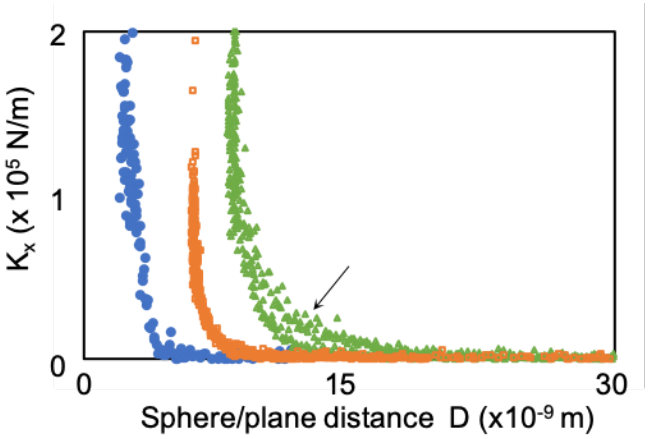

Fig. 4: Evolution of the tangential stiffness, K_x, as a function of the distance D, for hexadecane (blue circle), Pol-Carbox + hexadecane (orange square) and Pol-Amine + hexadecane (green triangle). The arrow indicates the existence of hysteresis between loading and unloading for Pol-Amine + hexadecane.

A time evolution/history dependence was observed: as the number of loading and friction tests increased, increases in hysteresis during loading/unloading as well as in the value of adhesive force, up to 0.15 mN, were detected. This is associated with an increase in film thickness to $2L_c$(1mN) = 7 nm. These findings are in good agreement with previous results obtained on hexadecane and dodecane [30].

Polymer Pol-Carbox - carboxylic acid anchor

The addition of large polymeric molecules to the hexadecane solvent modifies its behavior. The immobile surface layer that shifts the flow conditions can be measured by extrapolation, and corresponds to a thicker value, with L_H = 7 nm. In addition, the plot of the reciprocal of the normal damping deviates from the calculated damping with a viscosity of 3.5 mPa.s for distances smaller than 20 nm, as shown in **Fig 2a**. This behavior can be interpreted with the existence of an effective viscosity gradient from the surface to the bulk, resulting from a

monomer-concentration gradient due to the molecular adsorption on the surface [15-16]. This behavior can be modeled to a first approximation as a multi-layer interfacial film [16] composed of two layers of infinite viscosity, of thickness $L_H' = 5.6 \pm 0.3$ nm, on each surface, covered by a thinner layer, of viscosity 5 mPa.s and thickness 4.3 nm. L_H' corresponds to the immobile layer in the case of polymers. The covered surfaces are then separated by the bulk fluid of viscosity 3.5 mPa.s (see **Fig 2b and the inset**). This behavior was reversible during loading and unloading, and was independent of the time and the number of squeeze and friction experiments.

As confinement increased, below a separation distance of 10 nm, the normal force F_z/R curve increased smoothly and without detectable hysteresis. The force was purely repulsive as presented in **Fig 3**. The application of the Alexander-de Gennes model [34] to the onset of repulsion data, before the occurrence of any elastic deformation of the solids, provides a length of first repulsion, h, of about 5.2 ± 0.5 nm and a chain separation, L, of 1 ± 0.2 nm. These values are very small compared to the diameter of the poly(dodecyl methacrylate) (ca. 2nm). However, the Alexander-de Gennes theory assumes that the polymers have negligible diameter, which is clearly not the case here. If we account for the thickness of the chains, we reach a surface coverage on the order of 0.25 chain/nm^2 (i.e. ca. 2 nm chain separation) which is still a high coverage, and comparable to systems in which the films were prepared by grafting from the surface [17, 35].

This value of h is smaller than L_H but of the same order of magnitude as L_H'. This would confirm the existence of a multilayer film.

An elastic wall of thickness $2L_c$ (at 3mN) was measured as 6.3 ± 0.5 nm at a mean contact pressure of 45 MPa. The evolution of the Fz/R=f(D) plot, above 0.12 N.m, suggests a high stiffness of the interfacial film in the z direction. The tangential stiffness started increasing at a separation distance of 8.6-9 nm. Compared to the base-oil behavior, the tangential stiffness is lower, at around 70 000-90 000 N/m at the maximum normal force (see **Fig 4**). However, due to the thicker film, it showed a higher elastic shear modulus, equal to 7.1 MPa (assuming infinitely rigid substrates) or 8.7 MPa accounting for the solid elasticity (see **Table 2**).

Polymer Pol-Amine – primary amine anchor

The trend observed in the case of the addition of Pol-Amine (with the amine anchor) is similar to that seen for Pol-Carbox. The viscosity at large separation distance is 3.7 mPa.s, consistent with that of a dilute solution in hexadecane, and a L_H value of 21.5 nm can be obtained by extrapolation, despite a divergence of the reciprocal of the damping in the experimental data from the theoretical line, as soon as a separation distance 60 nm is reached (see **Fig 2a**). A similar interpretation as above can be made, although the model does not yield a unique solution due to the early and progressive deviation from the theoretical line: a reasonable model of the experimental data provides an immobile layer of L_H'= 10 nm of infinite viscosity, covered by a 13.5 nm-thick layer of viscosity 25 mPa.s before reaching the bulk solution (see **Fig 2b**).

This approach confirms the existence of a more viscous layer on the surface, which extends to the bulk over a rather large distance.

This behavior was reversible during loading and unloading and was independent of time, and the number of squeeze tests and friction experiments.

As confinement increased, starting from a large separation distance, the normal force was purely repulsive and hysteresis between loading/unloading was detected, as shown in **Fig 3**.

This hysteresis diminished with successive loading/unloading tests. The repulsive force was detected as the separation distance reached 2h, (h, L) decreasing from (30 nm, 6 nm) to (22 nm, 4 nm), as the number of squeeze tests increased. This tends to indicate that the block anchor was not fully attached to the surface and that the oleophilic block was rather extended into the bulk fluid at first. Another explanation could involve the presence of micelles, as suggested in **Table 1**, which would deform and reorganize in the vicinity of the surface. This evolution was associated with a decrease in the value of the elastic wall at 3 mN (i.e. 45MPa), $2L_c$ varies from 13 nm to about 8.6 nm.

Fig 4 shows that little hysteresis was measured in the evolution of the tangential stiffness between loading and unloading, in agreement with the normal force evolution. At 45 MPa, the confined layer had an elastic tangential stiffness of around 135 000 – 173 000 $N.m^{-1}$, resulting in an elastic shear modulus of 26 MPa (45 MPa if taking the solid elasticity into account): the discrepancy between these two G values showed that the elasticity of this adsorbed layer was not negligible compared to that of the solids, resulting in a mechanical coupling.

Table 2: Characteristic values of thickness and distances relative to the molecular organization and mechanical characterization of the adsorbed confined interfacial film in terms of elastic shear modulus, G, at 3 mN i.e. 44-45 MPa. * indicates '*stable*' values, measured after a series of loading/unloading cycles.[1)] derived from QCM (see **Fig. 1**), [2)] derived from inverse damping measurement (see **Fig. 2**), [3)] derived from normal force measurement (see **Fig. 3**), [4)] calculated from tangential stiffness shown in **Fig. 4**.

Fluid	Hexadecane	Pol-Carbox + hexadecane	Pol-Amine + hexadecane
[2)] L_H (nm)	1.35	7	21.5
[2)] L_H' (nm)		5.6	10
[1)] QCM film thickness (nm)		5.5 ± 0.4	9.3 ± 0.5
[3)] h (nm)		5.2 ± 0.5	22*
[3)] L (nm)		1 ± 0.2	4*
[3)] $2L_c$ [at F_z=1mN] (nm)	2.5	6.4 ± 0.5	8.6*
[3)] $2L_c$ [at F_z=3mN] (nm)	2	6.3 ± 0.5	8.6*
[4)] G ($x10^6$ Pa) [28]	4.3 ± 0.2	7.1 ± 0.1	26 ± 3
[4)] G ($x\ 10^6$ Pa) [32]	6.9 ± 0.2	8.7 ± 0.1	45 ± 3

Discussion of the structuring observed at large distance

The QCM-D are consistent with the damping evolution measured on the ATLAS molecular tribometer. The large shift in dissipation observed for both polymer solutions in the adsorption step can indeed result from two contributions: either a change in bulk viscosity or/and an interaction between the polymers adsorbed on the surface and those in solution.

This shift was larger for Pol-Amine than for Pol-Carbox. In addition, polymer Pol-Amine showed a distinct ΔFn/n signal: after an initial rapid adsorption, a slower process leading to a decrease in the frequency shift occurred. This is characteristic for vesicle adsorption and rearrangement phenomena [18, 25]. This observation was consistent with the dynamic light scattering (DLS) measurement, which gave a value of $2R_H$ of 44 nm for polymer Pol-Amine—much larger than the size of the individual copolymer coil in bulk solution. This would indicate that, despite hexadecane rinsing, some micelles might have remained intact on the surfaces (due to the interactions between polymer chains), explaining both the residual damping observed with the QCM and the damping evolution. This would also be consistent with the interpretation of multilayered structuring at large distances.

In addition, raw QCM data were processed assuming a density of 0.77 $g.cm^{-3}$ as with the bulk liquid [18], allowing one to estimate adsorbed film thickness of 5.5 nm ± 0.4 nm and 9.3 nm ± 0.5 nm on the surface, for polymers Pol-Carbox and Pol-Amine, respectively. These two values were very close to the modelled immobile layer L_H' and to the measured distance of onset of repulsion.

Discussion on the molecular organization during confinement, once pressure was applied

According to the literature [34, 36-37] for homopolymers (not brushes), $L_H/2R_H$ is close to 1. For both polymer solutions, we obtained L_H values smaller than $2R_H$ measured by DLS, indicating that solution structures are being broken up upon adsorption. The DLS measurements correspond most likely to the presence of large micelles, and the hexadecane rinsing steps are expected to have removed most of these structures.

In addition, for polymer Pol-Carbox, the Alexander-de Gennes value of L, the estimated end-chain separation distance between the polymer chains, was calculated to be about 1 nm. As discussed above, this translates into a 2 nm chain separation, and thus one can consider that this anchor block of copolymer is likely to form a flat film on the surface [38]. The value of h, the distance of onset of repulsion, of about 5 nm is of the same order as L_H', confirming the dense polymer coverage.

For polymer Pol-Amine, the few micelles still present in the bulk solution could be displaced during the quasi-static squeeze, explaining both the large distance of onset of repulsion, L being larger than the extended length of the block copolymer, and the normal compliance of the film during the first loading and the time evolution of F_z/R-D plot. The very slow loading velocity would allow the few micelles to flow away, leaving mainly some adsorbed block copolymers on the surface and a few micelles. This seems to be confirmed by the evolution of the tangential stiffness (see **Fig 4**).

In terms of confined film thickness, the values of $2L_c$, 6.3 nm and 9 nm, for Pol-Carbox and Pol-Amine, respectively, were much larger than for hexadecane and smaller than the extended length of the oleophilic block. Associated with the values of chain-end separation, this suggests that the opposing adsorbed layers were interpenetrating. This interpenetration would result in a higher tangential stiffness, than that expected from a repulsive brush configuration, consistent with our observations. In particular, the onset of increase in tangential stiffness reflects the beginning of the interpenetration. For polymer Pol-Amine, the time evolution of the F_z/R-D plot, the thicker films and the higher elastic shear modulus all tend to indicate more disorder in the molecular organization, compared to the situation for polymer Pol-Carbox—disorder that could be attributed to the presence of some isolated micelles.

Molecular organizations resulting from these molecular architecture and surface interactions, are schematically presented respectively in **Fig 5**.

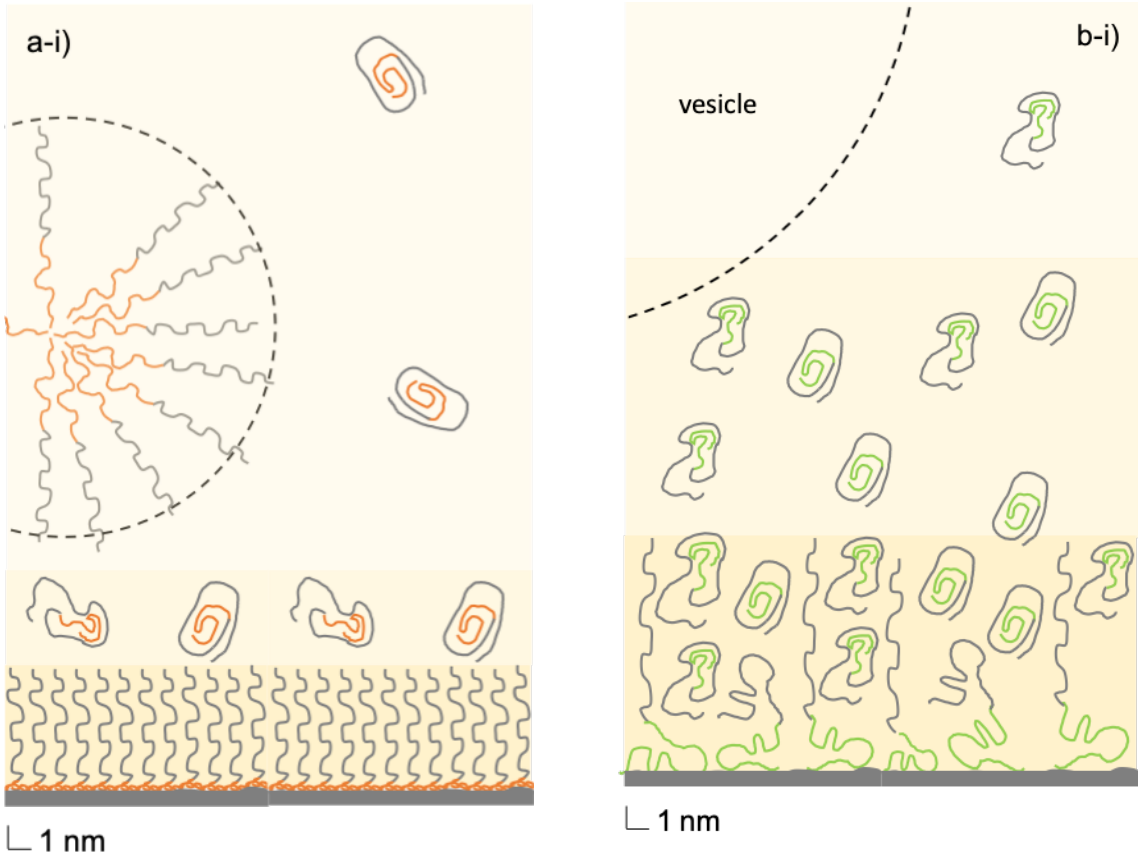

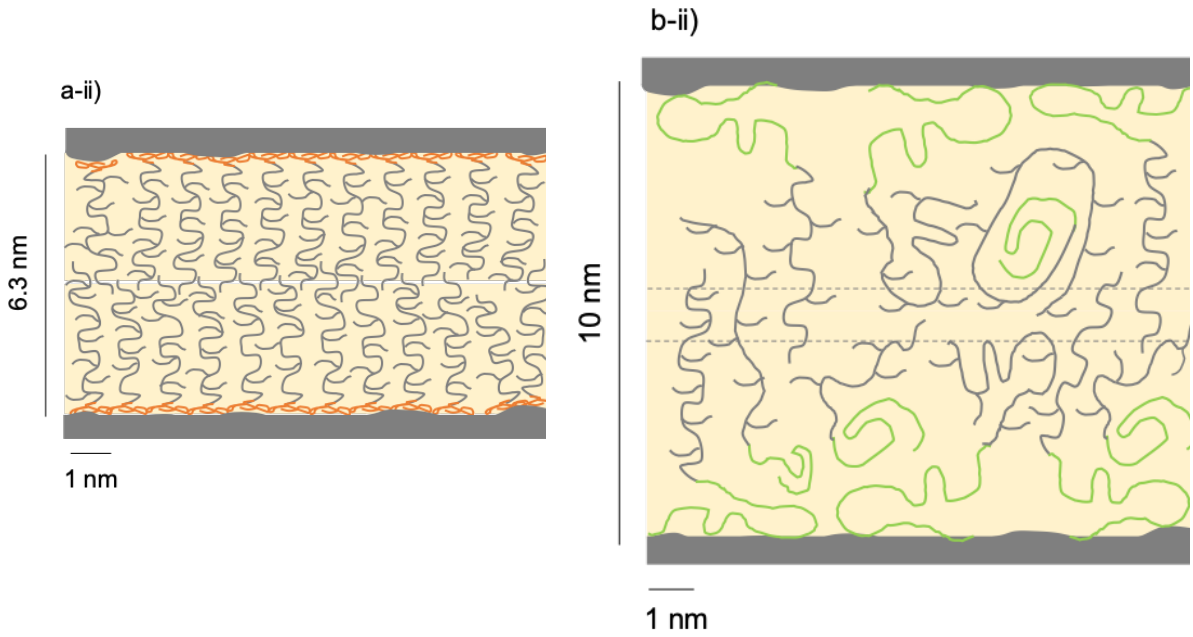

Fig. 5: Schematic of the molecular organization deduced from the combined ATLAS and QCM analysis for (a) Pol-Carbox + hexadecane and (b) Pol-Amine + hexadecane when the surfaces are apart (i) and contacting (ii). For the sake of clarity, in i) none of the side chains and in ii) only 20% of the side chains have been shown.

Boundary-film friction

Velocity dependence

The adsorbed Pol-Amine and Pol-Carbox layers were brought into contact under a constant normal force, at either 1 mN or 3 mN, and sheared at various sliding velocities. The friction force was measured as proportional to the normal force, up to 3 mN, at constant sliding velocity, following classical Amontons-Coulomb behavior, for all the considered sheared layers (pure hexadecane and polymers Pol-Amine and Pol-Carbox). **Fig 6** presents the evolution of the friction vs the sliding velocity.

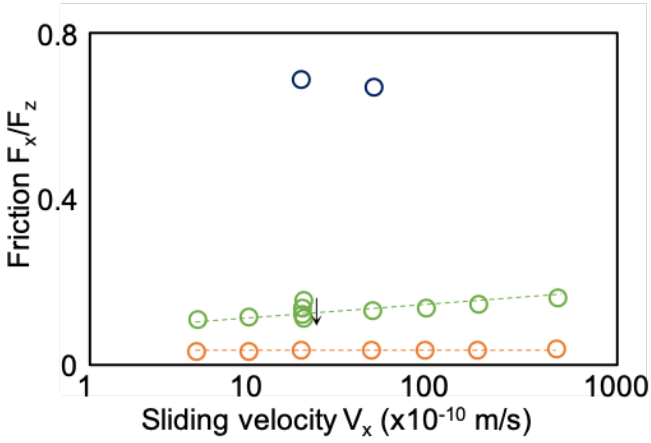

Fig. 6: Friction evolution vs sliding velocity for hexadecane (blue), Pol-Amine adsorbed films in contact (green) and Pol-Carbox adsorbed films in contact (orange). The arrow indicates the decrease in friction for successive friction loops at the same sliding velocity.

In the case of hexadecane, a high friction value, F_x/F_z, above 0.6, was detected, independent of the normal force, in agreement with previous results on hexadecane and dodecane [11]. This value was significantly larger than the theoretical value calculated considering the shear of a piezoviscous fluid layer of hexadecane under a contact pressure of 45 MPa.

In the case of polymer Pol-Amine, the friction was lower, at around 0.15-0.2. It was observed that the friction increased logarithmically with sliding velocity. The tangential stiffness was almost constant until a sliding velocity of 4 $nm.s^{-1}$, before decreasing slightly as the sliding velocity increased (see **Fig. 7**). Friction, Fx/Fz, diminished as the number of friction loops increased, for instance from 0.15 to 0.11 at a sliding velocity of 1.6 nm/s, associated with a slight diminution of the film thickness (about 1 nm).

In the case of polymer Pol-Carbox, a much lower friction coefficient, Fx/Fz, was reached at 0.03-0.04 with a very slight velocity-strengthening effect. The film thickness was constant and

the tangential stiffness decreased as the sliding velocity increased above 8 nm.s^{-1}. No significant effect of number of friction loops was observed.

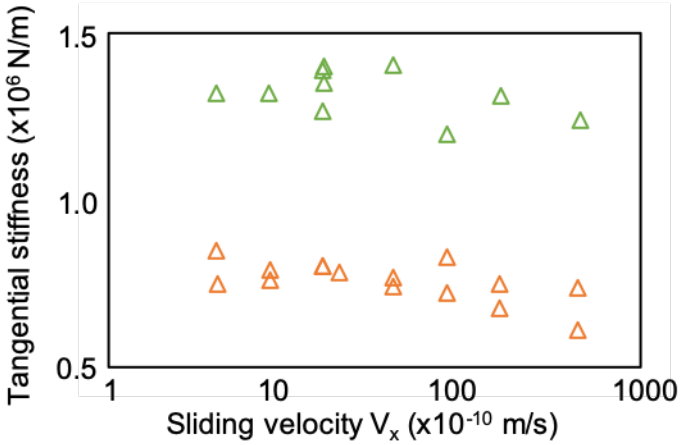

Fig. 7: Tangential stiffness evolution vs sliding velocity for Pol-Amine adsorbed films in contact (green) and Pol-Carbox adsorbed films in contact (orange).

Friction mechanisms

Two aspects will be discussed: the overall level of friction and the velocity dependence.

For Pol-Amine adsorbed layers, the overall decrease in friction level as the number of loops increased was associated with a slight decrease in the tangential stiffness level. This simultaneous evolution of friction and tangential stiffness (measured independently) confirmed the role of the boundary layer elasticity in the friction response.

The decrease in friction was also associated with a more pronounced diminution in the threshold distance, X*, by 25% at a sliding velocity of 1.6 nm/s over 4 friction loops (see **Fig. 8**). This critical sliding distance, X*, defined as: $X^* = F_x/K_x$, at first equal to 3.4 nm, can be interpreted as the distance required to switch from partial to total sliding [39-40] i.e. the distance required to switch from largely chain-tilting to total-sliding behavior. Its diminution tends to indicate a

molecular reorganization of the interfacial film under shear. It is noteworthy that these values of X* are of the same order of magnitude as the distance between end-chain separation, L.

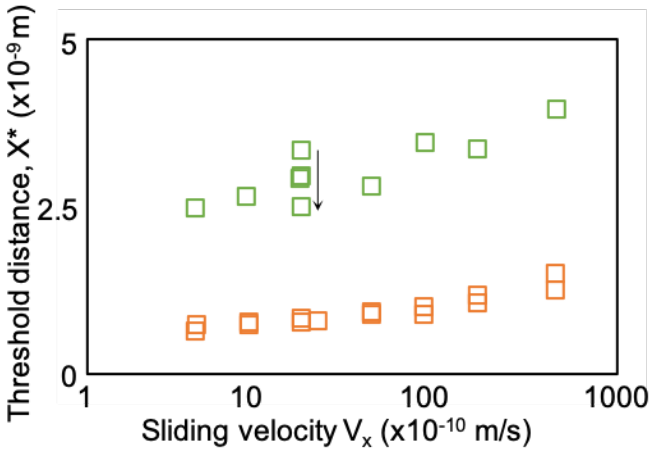

Fig. 8: Threshold distance, X*, vs sliding velocity for Pol-Amine adsorbed films in contact (green) and Pol-Carbox adsorbed films in contact (orange). The arrow indicates the dependence of X* on the number of loops.

The velocity dependence, however, reflects another, combined mechanism. Previous work [16, 40-41] has established that friction results from the dynamics of junctions formed between the two boundary layers in contact, i.e. the equilibrium between formation and rupture kinetics. In this context, the logarithmic dependence can be interpreted as a friction regime in which the junction-rupture process competes with thermal mechanisms with lowered activation barriers [16]:

$$F_x = \frac{\pi . a_H^2 . k . T}{\gamma . \delta A} . Ln(\frac{V_x}{V_0})$$

with F_x the friction force, a_H the Hertz contact radius, γ the thickness of the interpenetration zone, δA the mean area of a junction, $\gamma.\delta A$ corresponding to an activation volume, and V_0 a critical velocity defined as: $V_0 = \frac{k.T}{\gamma.\delta A} . \frac{D}{G.\tau_0}$ with D the film thickness, G the elastic shear modulus and τ_0 the mean time to break a junction.

The application of this model to our experimental data for Pol-Amine gives a value of activation volume, $\gamma.\delta A$, of 8 nm^3 and a mean time to break the junction, τ_0, of 5000 s. This very large value of time can be attributed to the high contact pressure, 45MPa, considered here, and to the relatively large critical distance, X*, of about 3 nm.

X* can be calculated over the whole range of sliding velocity and it increases with the velocity, from 2.5 nm to 4 nm (see **Fig. 8**). Considering that the activation volume is constant over the considered range of velocity, and assuming that X* is related to the average size of the junction, [5], this would result in an interpenetration zone of about 1 nm in thickness, consistent with the film-thickness measurement and the model described in **Fig 5b-ii**. This large degree of interpenetration would also contribute to increasing the mean time to break a junction. In addition, it can be seen that the interpenetration thickness decreases from 1.3 nm to 0.5 nm as the sliding velocity increases, indicating a small lift effect.

It is noteworthy that this model assumes a negligible viscoelastic contribution of the boundary film itself and that friction dissipation only occurs at the interface between the two boundary layers. This strong assumption could lead to an overestimate of the mean time to break a junction.

In the case of Pol-Carbox, the overall lower level of friction can be attributed to a combination of a lower tangential stiffness and a shorter critical distance X* of around 0.8 nm. This is characteristic of a well-organized boundary layer, as previously hinted at by the film-formation analysis. The almost constant friction can be accounted for by the previous model: it also predicts a friction regime in which the number of linked junctions is almost constant, [40-41] due to a slow molecular link formation. X* also increased as the sliding velocity increased, from 0.6 to 1.2 nm, as shown in **Fig. 8**. Once again, transient-friction overshoots were observed at each change in velocity and at the onset of sliding after stopping, supporting the multi-contact

interpretation [40]. Regardless of the number of loops, the degree of organization appeared to be stable, most likely due to strong surface anchoring.

Conclusions

Film formation and friction mechanisms were investigated for two polymer-brush-based friction modifiers in oil. The role of the anchor chemistry (carboxylic acid vs primary amine) was assessed, while keeping the molecular architecture constant in terms of block oleophilic/oleophobic copolymer structure and length.

For both polymers, we showed the existence of an adsorbed boundary layer on the surface. This boundary layer presented a complex structure, which can be mechanically described as a gradient of viscosity from the surface to the bulk. This structuring could be related to a brush-like film, with different anchor-surface-coverage ratio, to which micelles and/or vesicles are loosely attached, coexisting with those in the bulk due to the solubility of the block copolymer in oil.

Once brought into contact, these layers exhibited a repulsive normal force at relatively large separations, consistent with the length of the chain. Low or no hysteresis was observed during approach/retraction. Once compressed under few MPa, the brush-like layers behaved as an elastic wall of nanometric thickness and with a moderately high elastic shear modulus.

This mechanical behavior resulted in a friction behavior that was partially governed by the elasticity of the layer and partially by the dynamics of the junctions formed between the two layers within the interfacial zone. The friction dynamics with time and with sliding velocity were accounted for by the evolution of the junction size and the interpenetration thickness.

We have demonstrated that changing the anchor chemistry controlled the final ordering in the oleophilic boundary layer. The stability of the surface anchoring governed the onset of repulsion. It also controlled the behavior of the surface/anchor interactions as a function of both time and friction history, i.e. the capacity of the layer to withstand shear. The higher molecular order in the layer formed by Pol-Carbox was then responsible for the drastic friction reduction observed. This was presumably by virtue of the stronger, bidentate interactions of -COOH with the metal, firmly anchoring the friction modifier to the surface.

AUTHOR INFORMATION

Corresponding Author

J. Cayer-Barrioz, Laboratoire de Tribologie et Dynamique des Systèmes, CNRS UMR 5513, Ecole Centrale de Lyon, 36 Avenue Guy de Collongue, 69134 Ecully Cedex, France

Juliette.cayer-barrioz@ec-lyon.fr

Author Contributions

The manuscript was written through contributions of all authors. All authors have given approval to the final version of the manuscript. All authors contributed to the experimental design. SD, TG and JCB carried out the experiments.

Funding Sources

IMOTEP Project, ADEME, France.

Acknowlegment

SD and JCB acknowledge the financial support of the Agency for the ecological transition (ADEME) through the IMOTEP project. SD and JCB are also grateful to Dr Morgado for his help in preparing the surfaces.

References

1. Reynolds, O. On the Theory of Lubrication and its Application to Mr. Beauchamp Tower's Experiments, including an Experimental Determination of the Viscosity of Olive Oil. *Proc. R. Soc. London* **1886**, 191-203.
2. Hardy, W. B.; Doubleday, I. Boundary Lubrication - The Paraffin Series. *Proc. R. Soc. London,* Ser. A **1922**, 100, 550–574.
3. Georges, J.M.; Tonck, A.; Mazuyer, D. Interfacial Friction of Wetted Monolayers. *Wear* **1994**, 175, 59-62.
4. Lundgren, S. M.; Ruths, M.; Danerlöv, K.; Persson, K. Effects of Unsaturation on Film Structure and Friction of Fatty Acids in a Model Base Oil. *J. Colloid Interface Sci.* **2008**, 326, 530–536.
5. Mazuyer, D.; Cayer-Barrioz, J.; Tonck, A.; Jarnias, F. Friction Dynamics of Confined Weakly Adhering Boundary Layers. *Langmuir* **2008**, 24, 3857–3866.
6. Campen, S.; Green, J.; Lamb, G.; Atkinson, D.; Spikes, H. On the Increase in Boundary Friction with Sliding Speed. *Tribol. Lett.* **2012**, 48, 237–248.
7. Simic, R.; Kalin, M. Adsorption Mechanisms for Fatty Acids on DLC and Steel Studied by AFM and Tribological Experiments. *Appl. Surf. Sci.* **2013**, 283, 460–470.
8. Spikes, H.A. Friction Modifier Additives. *Tribol. Lett.* **2015**, 60: 5.
9. Crespo, A. ; Morgado, N. ; Mazuyer, D ; Cayer-Barrioz, J. Effect of Unsaturation on the Adsorption and the Mechanical Behavior of Fatty Acid Layers. *Langmuir* **2018**, 34, 4560-4567.
10. Abouhadid, F. Aspects Moléculaires du Frottement Limite: Couplage entre Structure des Additifs et Physico-Chimie des Surfaces. ECL PhD Thesis, 2021LYSEC48, **2021**.

11. Abouhadid, F.; Crespo, A.; Morgado, N.; Mazuyer, D.; Cayer-Barrioz, J. Friction Laws for Saturated/Unsaturated Fatty Acid Layers. *Tribol. Lett.* **2021**, 69:46.

12. Nalam, P.C.; Pham, A.; Veronica Castillo, R.; Espinosa-Marzal, R.M. Adsorption Behavior and Nanotribology of Amine-based Friction Modifiers on Steel Surfaces. *J. Phys. Chem. C* **2019**, 123, 13672-13680.

13. Guangteng, G.; Smeeth, M.; Cann, P.M.; Spikes, H.A. Measurement and Modelling of Boundary Film Properties of Polymeric Lubricant Additives. *Proc. Inst. Mech. Eng. Part J, J. Eng. Tribol.* **1996**, 210, 1–15.

14. Malosse, P. Contribution des Modificateurs de Frottement à la Lubrification des Transmissions Manuelles. Une Approche Multi-Echelles. ECL PhD Thesis, ECL2002-27, **2002.**

15. Cayer-Barrioz J, Mazuyer D, Tonck A, Yamaguchi E. Drainage of a Wetting Liquid: Effective Slippage or Polymer Depletion? *Tribol. Lett.* **2008**, 32: 81-90.

16. Cayer-Barrioz J, Mazuyer D, Tonck A, Yamaguchi E. Frictional rheology of a confined adsorbed polymer layer. *Langmuir* **2009**, 25(18) 10802-10810.

17. Bielecki, R. M.; Crobu, M.; Spencer, N. D. Polymer-Brush Lubrication in Oil: Sliding beyond the Stribeck Curve. *Tribol. Lett.* **2013**, 49, 263–272.

18. Gmür, T. Polymeric Friction Modifiers in Oil: Synthesis, Adsorption and Tribological Evaluation, ETH Zürich PhD Thesis, ETH27395, **2021**.

19. Gmür, T.A.; Mandal, J.; Cayer-Barrioz, J.; Spencer. N.D. Towards a Polymer-Brush-Based Friction Modifier for Oil. *Tribol. Lett.* **2021**, 69:124.

20. Georges, E.; Georges, J.M.; Diraison. C. Rheology of Olefinic Copolymer Layers Adsorbed on Solid Surfaces. Tribol. Trans. 1996, 39:3, 563-570.

21. Müller, M.; Topolovec-Miklozic, K.; Dardin, A.; Spikes, H.A. The Design of Boundary Film-Forming PMA Viscosity Modifiers. Tribol. Trans. 2006, 49, 225-232.

22. Fan, J.; Müller, M.; Stöhr, T.; Spikes, H.A. Reduction of Friction by Functionalised Viscosity Index Improvers. Tribol. Lett. 2007, 28: 287-298.

23. Pujari, P.S.; Scheres, L.; Marcelis, A.T.M.; Zuilhof, H. Covalent Surface Modification of Oxide Surfaces. *Angewandte Chemie* **2014**, 53(25), 6322-6356.

24. Sauerbrey, G. Verwendung von Schwingquarzen zur Wägung dünner Schichten und zur Mikrowägung. *Zeitschrift für Phys*. **1959**, 155, 206–222.

25. Reviakine, I.; Johannsmann, D.; Richter, R.P. Hearing What You Cannot See and Visualizing What You Hear: Interpreting Quartz Crystal Microbalance Data from Solvated Interfaces. *Anal*. *Chem*. **2011** 83, 8838–8848.

26. Crespo, A. Compréhension de la Tribologie des Films Limites: de l'Organisation Moléculaire à la Réponse en Frottement. ECL PhD Thesis, 2017LYSEC21, **2017**.

27. Crespo, A.; Mazuyer, D.; Morgado, N.; Tonck, A.; Georges, J.- M.; Cayer-Barrioz, J. Methodology to Characterize Rheology, Surface Forces and Friction of Confined Liquids at the Molecular Scale Using the ATLAS Apparatus. *Tribol*. *Lett*. **2017**, 65, 138.

28. Mazuyer, D.; Tonck, A.; Cayer-Barrioz, J. Friction Control at the Molecular Level: From Superlubricity to Stick-Slip; Erdemir, A., Martin, J.-M., Eds.; Elsevier Science B.V.: Amsterdam, **2007**, 397–426.

29. Ducolombier, D.; Zhou, H.; Boned, C.; Peyrelasse, J.; Saint-Guirons H.; Xans, P. Pressure (1-1000bars) and Temperature (20-100°C) Dependence of the Viscosity of Liquid Hydrocarbons. *J*. *Phys*. *Chem*. **1986**, 90, 1692-1700.

30. Tonck, A.; Georges, J. M.; Loubet, J.L. Measurements of Intermolecular Forces and the Rheology of Dodecane between Alumina Surfaces. *J*. *Colloid Interface Sci*. **1988**, 126, 150–163.

31. Heuberger, M.; Zach, M.; Spencer, N.D. Density Fluctuations Under Confinement: When is a Fluid Not a Fluid? *Science* **2001**, 292(5518), 905-908.

32. Gacoin, E.; Fretigny, C.; Chateauminois, A.; Perriot, A.; Barthel, E. Measurement of the Mechanical Properties of Thin Films Mechanically Confined within Contacts. *Tribol. Lett.* **2006**, 21, 245– 252.

33. Bec, S.; Tonck, A.; Georges, J.M.; Yamaguchi, E.S.; Ryason, P.R. Surface Force Apparatus Studies of Adsorbed Borate Films, *Tribol. Trans.* **2003**, 46:4, 522-533,

34. Georges E, Dispersion et forces de surfaces dans les hydrocarbures, ECL PhD Thesis, 96.35, 1996.

35. Kang, C.; Crockett, R.; Spencer, N.D. The Influence of Surface Grafting on the Growth Rate of Polymer Chains. *Polym. Chem.* **2016**, 7, 302.

36. Georges, J.M.; Millot, S.; Tonck, A.; Coy, R.C.; Schlijper,A.G.; Williamson, B.P. Nanorheology of Polyisoprene Solutions Confined between Two Solid Surfaces. Tribology for Energy Conservation, edited by D. Dowson, **1998** Elsevier Science B.V. 51-62.

37. Cohen Stuart, M.A.; Waajen, F.H.W.H.; Cosgrove, T.; Vincent, B.; Crowley T.L. Hydrodynamic Thickness of Adsorbed Polymer Layers. *Macromolecules* **1984**, 17, 1825-1830.

38. Marques, C.M.; Joanny, J.F. Block Copolymer Adsorption in a Nonselective Solvent, *Macromolecules* **1989**, 22, 1454-1458.

39. Mindlin, R.D. Compliance of Elastic Bodies in Contact. *J. of Appl. Mechanics* **1949**, 16, 259.

40. Frérot, L.; Crespo, A.; El-Awady, J.A.; Robbins, M.O.; Cayer-Barrioz, J.; Mazuyer, D. From Molecular to Multi-Asperity Contacts: How Roughness Bridges the Friction Scale Gap, arXiv:2111.13588 [cond-mat].

41. Chernyak, Y. B.; Leonov, A. I. On the theory of the Adhesive Friction of Elastomers. *Wear* **1986**, 108, 105–138.

Graphical abstract

7 x 3.2 cm2